

## Size calibration of self-assembled nanoparticles in a model of strained epitaxy with passive substrate

V. I. Tokar<sup>1,2</sup> and H. Dreyssé<sup>1</sup>

<sup>1</sup>*IPCMS-GEMM, UMR 7504 CNRS, 23, rue du Loess, F-67034 Strasbourg Cedex, France*

<sup>2</sup>*Institute of Magnetism, National Academy of Sciences, 36-b Vernadsky Street, 03142 Kiev-142, Ukraine*

(Received 27 July 2004; revised manuscript received 7 March 2005; published 14 July 2005)

We argue that a transient size calibration of self-assembled nanoparticles during strained epitaxy can be caused by forces interior to the growing islands without substrate-propagated interparticle interactions or intermixing with the substrate. The role of substrate in our mechanism is only to provide the intraparticle elastic strain. Our arguments are based on kinetic Monte Carlo simulations of the (1+1)-dimensional model of strained epitaxy of Ratsch and Zangwill (RZ) [Surf. Sci. **293**, 123 (1993)]. It has been found that while the energetics of the RZ model predicts indefinite ripening of the islands, in the simulations their linear dimensions saturated at intermediate times near some finite coverage-dependent values. Simultaneously statistical distributions of their widths and heights narrowed, thus providing improved size calibration. The size distributions obtained are qualitatively similar to those observed experimentally in the growth of ultrasmall supported metallic clusters. The applicability of the model to such systems is briefly discussed.

DOI: [10.1103/PhysRevB.72.035438](https://doi.org/10.1103/PhysRevB.72.035438)

PACS number(s): 68.65.-k, 81.07.-b, 81.16.Dn

### I. INTRODUCTION

In some heteroepitaxial systems the deposited atoms self-assemble into nanoparticles (or islands) with quite narrow distribution of their sizes<sup>1-5</sup> in contrast to the broad distributions usually observed both at the early stages of growth<sup>6</sup> as well as during the late stage ripening.<sup>7,8</sup> The phenomenon of size calibration (SC) attracted much attention recently because of its potentially rich technological applications in such fields as microelectronics<sup>9,10</sup> and catalysis.<sup>11,12</sup> Despite extensive research, however, the physics underlying this phenomenon, is not yet fully understood.

Because the SC was first discovered in coherent heteroepitaxial systems with appreciable misfit between the substrate and the overlayer,<sup>3-5</sup> it was suggested that the cause of the phenomenon should be sought in the physics of relaxation of the misfit strain.<sup>13,14</sup> This suggestion can be rigorously proved for one- and two-dimensional (1D and 2D) systems.<sup>14,15</sup> For example, in the 1D case the free ends of a chain pseudomorphically deposited on a substrate with a small lattice spacing can relax outwardly, thus providing a mechanism for the strain relief (see Ref. 13 and references therein). If the misfit is sufficiently large, the energy thus gained may exceed the energy of single interatomic bond.<sup>15</sup> In this case the long chains begin to separate into smaller pieces until some optimal length corresponding to the minimum energy per atom is reached,<sup>14</sup> thus providing a mechanism of SC.

In the case of growth in the direction normal to the surface, however, no similarly simple mechanism of the SC is known. Moreover, in the case of *isolated* islands simple scaling arguments show that the bulk binding energy which is proportional to the island's volume dominates over the surface relaxation energy, so the Ostwald ripening at the late stage of growth is inevitable.<sup>16,17</sup> Therefore, in order to explain the experimentally observed SC the interactions between the islands caused by the long range elastic forces

were invoked by some authors.<sup>17,18</sup> An alternative mechanism is based on the material transport between the wetting layer and the island.<sup>16</sup> That is, in both cases the explanation of the SC was sought in some agents which are external to the growing island.

The aim of the present paper is to show that SC can be achieved exclusively via the forces which are confined to the interiors of the island similar to the 1D- and 2D cases mentioned above. To this end in Sec. III we perform a kinetic Monte Carlo (KMC) simulation of the growth kinetics of self-assembled nanoparticles in the (1+1)D model of Ratsch and Zangwill<sup>13</sup> (RZ) which is briefly explained in Sec. II. The RZ model was chosen because it is based on the notion of the passive rigid substrate, i.e., no elastic force is transmitted from one island to another and, besides, the substrate atoms are immobile and their only role is to provide the binding and the misfit strain with the growing overlayer. The island size distributions obtained in our simulations are qualitatively similar to those observed experimentally in some experiments on heteroepitaxial growth.<sup>1,2,19,20</sup> In particular, in the growth of supported metallic clusters,<sup>1,2</sup> The applicability of the RZ model to such systems will be briefly discussed in Sec. IV.

### II. THE RATSCH-ZANGWILL MODEL

Let us consider a rigid 1D "surface" consisting of regularly spaced deposition sites on which the atoms are deposited in such a way that the solid-on-solid (SOS) condition is satisfied, i.e., each deposited atom should sit either on the surface or on another atom. In this rectangular geometry an arbitrary atomic configuration can be decomposed into rectangular blocks of size  $w \times h$ , where  $w$  is the width of the block measured in the number of atoms and  $h$  is its height. (We note that our definition of width  $w$  differs by 1 from that of Ref. 13.) Because of the lattice size misfit between the substrate and the growing overlayer,<sup>13</sup> the deposited atoms

try to relax the elastic strain caused by this misfit. The mechanism of relaxation is the same irrespective of whether the block is deposited on the substrate or on the top of a cluster. The only difference is in the misfit which weakens for higher layers in proportion to the relative elongation of the underlying layers due to their relaxation. The misfit can be defined blockwise, i.e., if the misfit with the underlayer is  $f_u^{(0)}$ , then the deposit on the top of the block under consideration will experience the misfit

$$f_u = \exp[-\Lambda h/(w-1)]f_u^{(0)}, \quad (1)$$

where  $\Lambda=3\pi/2$  is the relaxation length.<sup>13</sup> Thus, the misfit is exponentially small at the tops of tall islands and for each configuration can be calculated with the use of the above formula provided the misfit with the substrate  $f_{u=\text{substrate}}^{(0)}$  is known.

The energy of the configuration can also be defined blockwise with the energy of the block being equal to

$$E_{w \times h} = E_{\text{bond}} + E_{\text{elastic}} \\ = V_{\text{NN}}h(2w-1) + Af_u^2 \frac{(w-1)^2}{2\Lambda} \left[ 1 - \exp\left(-\frac{2\Lambda h}{w-1}\right) \right], \quad (2)$$

where  $A$  is an elastic constant,  $f_u$  is the misfit with the underlayer on which the block resides, and  $V_{\text{NN}}$  is an attractive interaction between nearest neighbor atoms. In this formula the Stranski-Krastanov growth mode is assumed with the wetting layer playing the role of the substrate,<sup>21</sup> so the atomic binding to the substrate and to the top of a cluster is assumed to be of the same magnitude.

The inevitability of the ultimate Ostwald ripening in this model can be easily shown at low temperature where the energy term in the free energy dominates. Thus if the misfit exceed the critical value<sup>15,21</sup> so that the atoms on the substrate self-assemble into size-calibrated islands of width  $w_0$  and height  $h_0$ , then this state is unstable with respect to the stacking of the islands into a pile of width  $w_0$  (in reality the optimum width of the pile will be different<sup>13</sup>). This is easily seen from the elastic term in Eq. (2) which is always positive and is diminishing in value because of the diminution of  $f_u$  in Eq. (1). This reasoning, in fact, is quite general and can be applied to any model based on the assumption of rigid substrate. It is based on the simple notion that the atoms on the top of a tall cluster deposited on a strained substrate are weakly influenced by the latter, so their growth should proceed as in the unstrained case, i.e., indefinitely. So at long times the growth should reduce to the conventional Ostwald ripening with a broad distribution of cluster sizes characteristic to it, as predicted by theory<sup>22</sup> and confirmed experimentally.<sup>7,8</sup>

Thus, it seems that the only possibility for the existence of the SC phenomenon is a transient calibration during some period between the initial stage of growth toward some optimum sizes (at this stage the size distribution is known to be broad<sup>6</sup>) and the final stage of the Ostwald ripening also characterized by broad size distributions. Such a possibility was suggested in Refs. 7, 13, and 2.

### III. THE KMC SIMULATION

In the standard experiment on heteroepitaxial growth the atoms are randomly deposited on the surface where they diffuse and attach to growing islands. The kinetics of the growth is defined by four major factors: by the rates of deposition, diffusion, and atomic capture and detachment by and from the islands.<sup>6</sup> These processes influence the island size distribution in different ways. The random deposition generally broadens the distribution because the attachment rate is weakly dependent on the island size.<sup>6</sup> On the other hand, given a broad size distribution, it is obvious that in order for a narrow distribution to arise the atoms should detach from islands of nonoptimal size in order to diffuse and attach to islands which are closer to the optimum size. Thus, the detachment rate governs the speed of the SC, provided the system admits such a regime. It is to be noted that in contrast to the external flux which can be tuned to practically any desirable value, the detachment rate depends on the interatomic interactions and at a fixed temperature is beyond our control and is very small at experimental temperatures of the order of a few hundred kelvins because interatomic interactions are of the order of 1 eV, i.e.,  $\sim 10^4$  K. Thus, the SC is controlled by the slow processes of detachment and it may be easily obscured by an inappropriately chosen deposition flux. For example, the KMC simulation of a (2+1)D model of strained epitaxy made in Ref. 21 did not show a SC in the vertical direction. The magnitude of the deposition flux was chosen by the authors to have a typical value used in real experiments. But because the model used was rather crude, *a priori* it is not clear that the flux value chosen was sufficiently small to not suppress the SC phenomenon. Such a possibility is well illustrated by the results of Ref. 23 where in the case of the 2D growth a radical narrowing of the size distribution was observed when the deposition flux was switched off.

Thus, it seems logical to study the SC in its pure form, i.e., in the absence of the deposition flux. In this case we can establish a characteristic time(s) controlling this phenomenon and then decide on the value of the deposition flux at which the SC can be observed during the conventional deposition experiment. Therefore, to minimize the number of parameters in our study we performed all simulations starting from the initial configuration obtained by the random deposition of atoms on the surface subject only to SOS restriction. We note that such a simulation not only can be of purely theoretical interest but may also model a possible experimental setup. The latter can be realized, e.g., through the initial deposition at low temperature where the atomic diffusion is negligible with subsequent annealing at an elevated growth temperature. The latter so-called postdeposition annealing technique was used, e.g., in Ref. 24 to study the Ostwald ripening of supported metallic clusters.

The assumptions of passive substrate and the absence of elastic interisland interactions can be realized in the growth of supported metallic clusters on insulating substrates.<sup>1</sup> Unfortunately, in the systems of this type that we are going to discuss the misfit strain is difficult even to define because the details of the coupling to the substrate are not known. It is most probable that the notion of coherent attachment is

meaningless here because the lattice parameters of corresponding materials are hugely different.<sup>1,2,31,32</sup> Therefore, we accepted a more phenomenological approach. By noting that the linear dimensions of the monolayer-high islands in Ref. 1 are about 7 atoms and having at our disposition the exact solution at finite temperature for 1D chains<sup>15</sup> we found that the choice  $Af_0^2 = |V_{NN}|/3$  provided the desired island sizes.

The choice of the parameter of the pair interatomic bonding  $V_{NN}$  is not an easy matter because, as is known, the interatomic interactions in metals strongly depend on the atomic coordination (see, e.g., Ref. 25 and references to earlier literature therein). We will continue the discussion of the coordination dependence of  $V_{NN}$  in Sec. IV while for the KMC simulations we will adopt the conclusions of Ref. 26 (where the supported Fe and Co clusters on an insulating substrate were considered) by taking the pair bonding between Fe and Co atoms as well as their binding to the substrate to be approximately equal to 1 eV.

The growth in Refs. 1 and 2 was performed at the room temperature and at 550 K, respectively. Therefore, most of our simulations were performed at the value of the parameter  $\beta = |V_{NN}|/kT$  equal to 30 which is similar to the values in the above experiments.

With the above parameters we performed KMC simulations by assuming activated dynamics with the hopping rate<sup>6</sup>

$$D = \nu_0 \exp[-(E_d - \Delta E)/kT], \quad (3)$$

where  $\nu_0$  is the attempt frequency,  $E_d$  the hopping barrier, and  $\Delta E$  the difference of energies of the configurations with and without the hopping atom.  $\Delta E$  was calculated with the use of Eqs. (1) and (2). The parameters  $\nu_0$  and  $E_d$  were considered to be configuration-independent constants and because their precise values are not known for the systems under consideration, we chose the parameter

$$\tau_0 = \exp(E_d/kT)/\nu_0 \quad (4)$$

to be the KMC time unit. Its physical value for the supported metallic clusters is estimated below.

Because of the low temperature chosen for the simulation, an event-based algorithm<sup>27</sup> was used. Simulations were performed on systems of length  $L = 2^{14} \approx 16\,000$  averaged over 60 seeds to gather sufficient statistics. The choice of the large system size was dictated by the number of parallel CPUs available to us. If this number can be increased or the number of seeds can be enlarged in some other way to provide similar statistics then the system size can be taken to be much smaller than above because no long range correlations were noted in the simulation data. The coverages studied were  $\theta = 0.25, 0.75$ , and 2. Time  $t$  in the simulations was measured in units of  $\tau_0$  which physically corresponds to the hopping rate of an atom which is laterally unbound.

The physical time interval corresponding to our simulation span of  $10^{14}\tau_0$  is not easy to define in view of the large scatter in the available data on the values of the diffusion barrier  $E_d$  and of the attempt frequency  $\nu_0$  in Eq. (3). Presumably, an absolute minimum at room temperature constitutes approximately 6 min if we take both parameters from Ref. 26 where the value of  $\nu_0 = 11$  THz corresponding to bulk Fe was proposed for use also for Fe on the surface. The



FIG. 1. Typical atomic configuration at the end of the simulation ( $t = 10^{14}$  of inverse hopping rate units) at the coverage  $\theta = 2$ . Black squares, the deposited atoms; gray squares, those of the substrate. A small portion of the simulated system of about 16 000 sites was chosen randomly with the only bias that the whole islands were visible.

lowest energy barrier for Fe diffusion was estimated to be 0.1 eV. In reality both the surface  $\nu_0$  and the barrier can be very different, so the only definite conclusion about our simulation span is that it is of macroscopic extent.

During the simulation at low temperature the clusters in a relatively short time ( $t < 10^{12}\tau_0$ ) self-assembled into nearly perfect rectangular islands similar to those shown in Fig. 1. Therefore, the statistical information was gathered in the form of the width-height pairs. The height was defined as the average over the width of the island at half its height. The data were collected with intervals  $\Delta t = 10^{12}\tau_0$ . The  $t = 0$  data are not presented in Fig. 1 because the  $h$  and  $w$  parameters as defined above are poorly suited to describe the initial ragged configuration.

Our main result is presented in Fig. 2 where the time dependence of average island height is presented together with the dispersion of the height distribution. As is seen, for each coverage studied the average height saturates at a value close to an integer number of layers. For coverages  $\theta = 0.25$  and 2 the widths of the height distributions also show saturated behavior while in  $\theta = 0.75$  case it is diminishing at large  $t$ . In our opinion, despite the similarity between the first and the third cases, the behavior of the  $\theta = 0.75$  curve together with the data on the width distributions and their dispersion shown in Figs. 3 and 4 allow us to speculate that the three cases correspond to qualitatively different stages of their evolution. Namely, in the case  $\theta = 0.25$  the system already reached its local equilibrium state because from  $t = t_{eq} \approx 5 \cdot 10^{13}\tau_0$  the height distribution is practically monodisperse ( $h = 1$  for the majority of islands) and the width distribution is

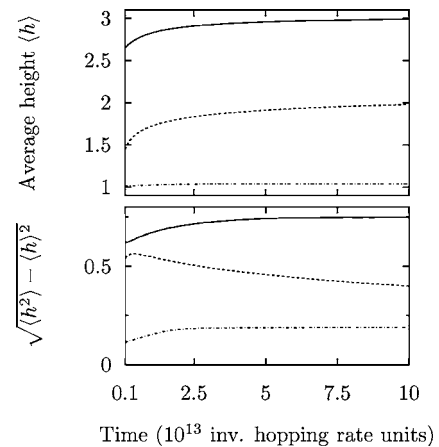


FIG. 2. Time dependences of average island height (upper panel) and the dispersion of the height distribution (lower panel) for  $\beta = V_{NN}/kT = 30$  and coverages  $\theta = 0.25$  (dash-dotted line), 0.75 (dashed line), and 2 (solid line).

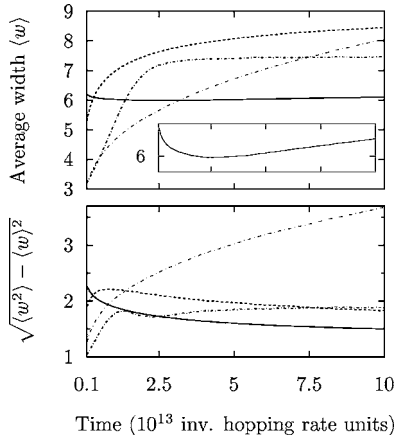


FIG. 3. Average width (upper panel) and the dispersion of the width distribution (lower panel) for the same coverages as in Fig. 1: dash-dotted lines correspond to  $\theta=0.25$ , dashed lines to  $\theta=0.75$ , and solid lines to  $\theta=2$ . In the case of  $\theta=0.25$  the line with shorter dashes corresponds to the RZ model. The line with the longer dashes correspond to the model with only NN interaction (i.e., no elastic relaxation) with  $V_{NN}/kT=27.5$  taken to be smaller than the corresponding quantity in the RZ case (i.e.,  $\beta=30$ ) to imitate the weakening of the NN interaction due to elastic forces. The inset in the upper panel shows the  $\theta=2$  curve magnified 5.5 times along the vertical axis to show the slow growth of the average length at large times.

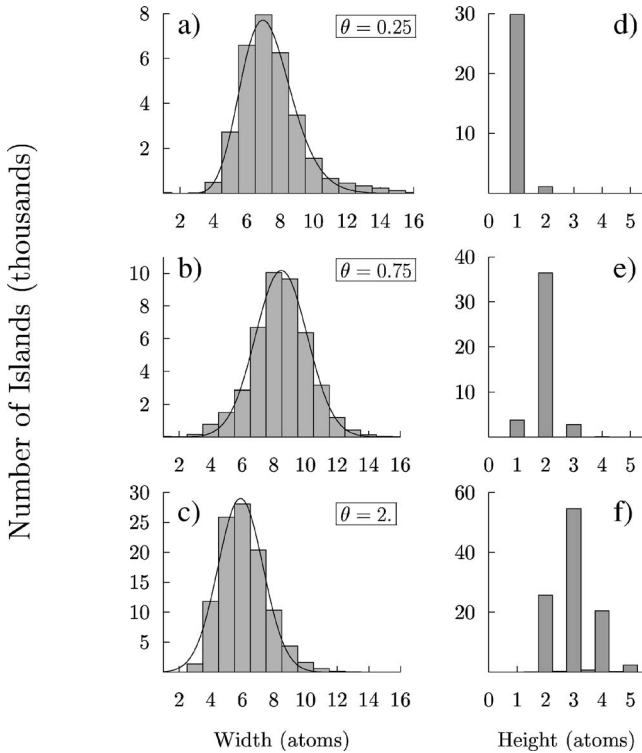


FIG. 4. Width (a)–(c) and height (d)–(f) distributions of self-assembled nanoislands for three coverages at  $t=10^{14}$  inverse hopping rate units. The vertical label on the left refers to all vertical axes. The solid lines in (b) and (c) are the Gaussian fit to the data while in (a) the solid line is the exact solution of the 1D model of Ref. 28. The data points at integer values of width were connected by splines for better readability.

well described by the equilibrium solution of Ref. 28. Because other parameters also do not show any considerable variation for  $t > t_{eq}$ , we may conclude that the system (quasi)equilibrates around this time.

In contrast, in the case  $\theta=0.75$  from Figs. 2 and 3 we see that the dispersions of the height and width distributions are monotonically diminishing while the average width is not yet fully saturated. From the value of the height dispersion and from Fig. 4(e) we see that the system is tending toward monodisperse distribution of heights as in the case  $\theta=0.25$  but in this case with  $h=2$ . Thus, one may expect that the quasiequilibrium state will be reached at some later time value larger than our maximum time  $t=10^{14}\tau_0$  but not too much larger because from the curves in the above figures it is seen that the saturation time is close. This is confirmed by the results shown in Fig. 5 where the simulation time span was enlarged tenfold.

From the above we conclude that the similarity of the behavior of the curves in Fig. 1 in the cases  $\theta=2$  and 0.25 is coincidental and does not mean that they reached the same evolution stage. On the contrary, we expect that the system in the former case is yet quite far from its quasiequilibrium state because the above tendency of going from lower to higher coverage suggest that the highest coverage corresponds to the highest equilibration time. In our opinion this is confirmed by the continuing diminution of the width distribution dispersion seen in Fig. 3 in the case  $\theta=2$ . Another argument is that the average height and width in the case of two lower coverages monotonically depend on the coverage, i.e., the higher coverage, the larger the quantities mentioned. This tendency is confirmed experimentally (see, e.g., Ref. 2). The highest coverage, however, violates this tendency in the case of the average width which is the smallest of the three. But from the inset in the upper panel of Fig. 3 we see that the average width in the  $\theta=2$  case is growing, though very slowly. Thus, we may assume that the  $\theta=2$  system has a

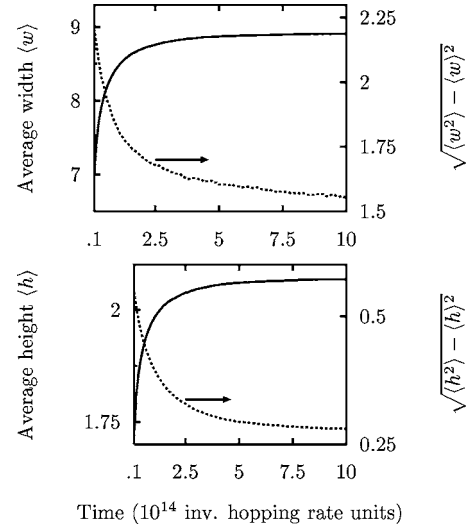


FIG. 5. Time dependence of average linear sizes of self-assembled islands (solid lines, left axes) and dispersions of their distributions (dotted lines, right axes) for coverage  $\theta=0.75$ . The inverse temperature parameter  $\beta$ , as well as the system size and the number of seeds, are the same as in previous figures.

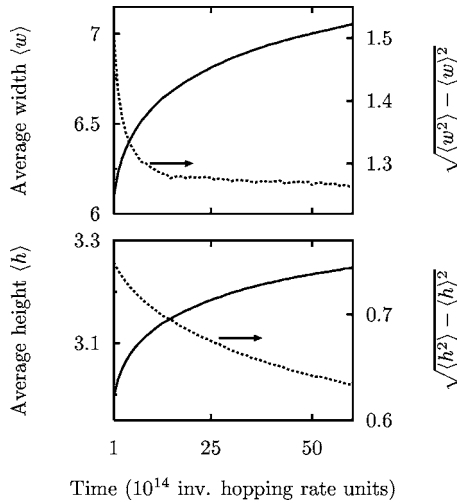


FIG. 6. Time evolution at coverage  $\theta=2$ . (For further explanations see the caption to Fig. 5.)

characteristic (quasi)equilibration time much larger than for the lower coverages. Indeed, in this case we were unable to reach the quasiequilibrium state even by extending our simulation span 60 times (see Fig. 6). However, the unsaturated growth of  $w$  and  $h$  seen in Fig. 6 is very slow, of the order of 10–15%. At the same time, the dispersions of both distributions continuously diminish. Thus, by arresting the evolution at a sufficiently late stage with a capping overlayer, as is often done experimentally, one can obtain an ensemble of quantum dots exhibiting good size calibration.

In Fig. 4 are shown the size distributions for all three coverages studied taken at  $t=10^{14}\tau_0$ . We note a striking similarity of these distributions to the experimental results presented in Fig. 1 of Ref. 1 and Fig. 3 of Ref. 20. Our height distributions are more peaked around the integer values of  $h$  than those of Ref. 1, but we attribute this to the absence of experimental errors in our data and, more essentially, to the idealized geometry used by us. For example, there is no way to have  $h < 1$  in our approach. But even more important is the kinetic nature of the SC phenomenon studied. Because of this various size distributions undergo qualitative changes during their evolution. In particular, the height distributions are much less peaked at the early stage of evolution when the islands have not yet achieved their almost impeccable rectangular geometry seen in Fig. 1.

We did not check the linear dependence of the island number on the coverage (also observed by the authors of Ref. 1) because the existence of such a dependence looks quite obvious at least for coverages lower than  $\theta=0.25$ . Indeed, because the islands are mainly monolayer high at  $\theta=0.25$ , the system is effectively one dimensional in which case the exact solution is known.<sup>28</sup> This solution tells us that the size-calibrated islands have coverage-independent average size. Thus, the linear dependence of their number on the coverage is guaranteed at least for  $\theta \leq 0.25$  but it is reasonable to assume that the dominance of the monolayer-high islands will continue for coverages appreciably larger than that value.

Unfortunately, our data are insufficient to draw any definite conclusions about the functional dependence of  $h$  on  $\theta$ .

But they definitely show that there is no any unique optimum island size as in the equilibrium case but that the transient equilibration takes place around some value defined by the quantity of the atoms available in the vicinity of a growing island and the kinetics. Also it is worth pointing out that our data are in qualitative agreement with Ref. 1 where the islands have approximately the same width for all coverages studied.

To conclude this section we note that the time dependences of the average width in Fig. 3 exhibits the self-limiting behavior observed experimentally in quantum dot systems.<sup>19,29</sup> Also, the islands in Fig. 1 quite often are separated by only a single vacant site and yet do not coalesce. This resistance to coalescence was observed experimentally in the growth of supported metallic clusters in Ref. 1 which means that the energetics of the RZ model may describe also such systems. Some theoretical arguments in favor of this suggestion (in addition to the qualitative agreement between our KMC data and the experimental data of Ref. 1) will be given in the next section.

#### IV. SUPPORTED CLUSTERS

The mechanism of the SC proposed in the present paper was designed with the aim to explain the experiments on self-assembly in systems with a passive substrate, i.e., those without noticeable interisland elastic interaction and without island-substrate intermixing. The intermixing can be avoided either by working at sufficiently low temperatures<sup>20</sup> or choosing a substrate-deposit pair with low chemical intermixing.<sup>1</sup> The interisland interaction can be avoided either by considering the systems with large island separation or with a sufficiently rigid substrate. The growth of the Co and Fe supported clusters in Ref. 1 satisfied the above conditions of the passive substrate.

In addition to the coherent structures, such as the ultrasmall quantum dots in Ref. 20, we hope that our approach can be also applicable to the self-assembly and SC of supported metallic clusters.<sup>1</sup> In this case the coherence of the substrate and the cluster is not guaranteed but our hope is based on the observation that if the kinetics is defined by the dependence of the island energy  $E_{island}(n)$  on the number of atoms  $n$ , as suggested in Ref. 14, then the specific mechanism responsible for the essential features of this dependence is not important. Indeed, the only information about the elastic forces the model contains is the parameter with the dimension of energy  $Af^2$  and the relaxation length  $\Lambda$ . But as formulated mathematically in Eqs. (1) and (2) these parameters may as well describe different physics.

For example, the curvature of the binding energy per atom  $E(n)/n$  for free  $Fe_n$  clusters calculated in Ref. 30 behaves in qualitatively the same way as the relaxation energy in the Frenkel-Kontorova model on which the RZ model is based,<sup>13</sup> as can be seen from the calculations of Ref. 15, for example. The  $Fe_2$  energy in Ref. 30 which should be associated with the relaxed NN interaction is about 4 eV, while the cohesive energy per bond in the bulk iron is about 0.7 eV. Thus, the most relaxed atomic configuration and the most compressed in the terminology of RZ model differ very significantly

which means that the effective “elastic” energy  $Af^2$  is large. Also the behavior of the energy during the growth in the normal direction should qualitatively correspond to that of the RZ model because the system saturates to its bulk properties, so the nonlinearity in the reduced energy  $E(n)/n$  curve should diminish, as can be seen from Fig. 4 of Ref. 30, thus imitating the weakening of misfit in our Eq. (1). Thus, the energetics of the RZ model may be qualitatively similar to the energetics of metallic clusters, with the metallic bonding phenomena playing the role of the misfit strain. The only problem is that for free clusters the curvature introduced by the band structure effects is insufficient to provide the minimum in the  $E(n)/n$  curve, or otherwise bulk metals would not exist. Here we may invoke the local minima in the dislocated islands<sup>31,32</sup> which provide the local minima in the reduced energy of the monolayer-high islands, which is sufficient for our purposes. This is more plausible in the case of ultrasmall nanoislands considered by us because in this case the local minima in the  $E_{\text{island}}(n)/n$  dependence are quite deep and well separated. In our opinion, this is confirmed by the qualitative similarity between our simulations and experimental results of Ref. 1.

We note that the RZ model approach does not contradict the notion of the magic numbers invoked in Ref. 1 to explain their experimental data. In this approach such numbers appear if the growth along the sequence of optimal clusters<sup>13</sup> proceeds in a layer-by-layer fashion. It is easy to see that when one layer is completed and another one begins to grow with an isolated atom being deposited on the top of the filled layer, one will obtain a large peak in the discrete second derivative in the cluster energy similar to those seen in Fig. 3 of Ref. 1. Similarly to the above figure we can see the enhancement of statistics of islands with completed layers in our Figs. 4(d)–4(f). Thus, while being devised for description of strained epitaxy, the RZ model may qualitatively describe energetics of supported metallic clusters as well, as the comparison of our simulation results with experimental data of Ref. 1 allows us to suggest.

## V. CONCLUSION

To sum up, in the framework of a simple model of strained epitaxy with the use of the KMC technique we have shown that in addition to the SC mechanisms proposed earlier and based on the influence of external factors on the growing island, such as the substrate-mediated elastic forces<sup>17,18</sup> or material exchange with the substrate,<sup>16</sup> there is the possibility of SC due to the internal interatomic interactions within the growing islands. The role of the substrate is only to provide an appropriate dependence of the cluster energy on the number of atoms. Because of this, the details of the attachment of the islands to the substrate may be not important for the SC and the theory proposed in the present paper can be applied in the situations where these details are not known, as is the case with the growth of supported metallic clusters. The mechanism considered above confirms the suggestion made by several authors<sup>2,7,13</sup> that the SC of self-assembled atomic clusters observed in some heteroepitaxial systems is a transient phenomenon which may be associated with a metastable state<sup>2,7</sup> having a finite lifetime. Thus we may speculate that the only essential requirement for our mechanism to be operative is the size and geometry dependence of the island free energy which should possess one or several local minima. The KMC simulations of the present paper give indirect evidence for the existence of such minima in the case of the RZ model. A rigorous confirmation of this hypothesis would require the computation of some nonequilibrium free energy of the system as proposed, e.g., in Ref. 33.

## ACKNOWLEDGMENTS

The authors acknowledge CNRS for support of their collaboration and CINES for computational facilities. One of the authors (V.T.) expresses his gratitude to University Louis Pasteur de Strasbourg and IPCMS for their hospitality.

<sup>1</sup>S. Gwo, C.-P. Chou, C.-L. Wu, Y.-J. Ye, S.-J. Tsai, W.-C. Lin, and M.-T. Lin, *Phys. Rev. Lett.* **90**, 185506 (2003).

<sup>2</sup>Z. Gai, B. Wu, J. P. Pierce, G. A. Farnan, D. Shu, M. Wang, Z. Zhang, and J. Shen, *Phys. Rev. Lett.* **89**, 235502 (2002).

<sup>3</sup>D. J. Eaglesham and M. Cerullo, *Phys. Rev. Lett.* **64**, 1943 (1990).

<sup>4</sup>Y.-W. Mo, D. E. Savage, B. S. Swartzentruber, and M. G. Lagally, *Phys. Rev. Lett.* **65**, 1020 (1990).

<sup>5</sup>S. Guha, A. Madhukar, and K. C. Rajkumar, *Appl. Phys. Lett.* **57**, 2110 (1990).

<sup>6</sup>C. Ratsch and J. A. Venables, *J. Vac. Sci. Technol. A* **21**, S96 (2003).

<sup>7</sup>S. Lee, I. Daruka, C. S. Kim, A.-L. Barabási, J. L. Merz, and J. K. Furdyna, *Phys. Rev. Lett.* **81**, 3479 (1998).

<sup>8</sup>S. H. Xin, P. D. Wang, A. Yin, C. Kim, M. Dobrowolska, J. L. Merz, and J. K. Furdyna, *Appl. Phys. Lett.* **69**, 3884 (1996).

<sup>9</sup>R. P. Andres, T. Bein, M. Dorogi, S. Feng, J. I. Henderson, C. P.

Kubiak, W. Mahoney, R. G. Osifchin, and R. Reifengerger, *Science* **272**, 1323 (1996).

<sup>10</sup>A. O. Orlov, I. Amlani, G. H. C. S. Lent, and G. L. Snider, *Science* **277**, 928 (1997).

<sup>11</sup>C. T. Campbell, *Surf. Sci. Rep.* **27**, 1 (1997).

<sup>12</sup>L. M. Molina and B. Hammer, *Phys. Rev. B* **69**, 155424 (2004).

<sup>13</sup>C. Ratsch and A. Zangwill, *Surf. Sci.* **293**, 123 (1993).

<sup>14</sup>C. Priester and M. Lannoo, *Phys. Rev. Lett.* **75**, 93 (1995).

<sup>15</sup>V. I. Tokar and H. Dreyssé, *Phys. Rev. B* **68**, 195419 (2003).

<sup>16</sup>L. G. Wang, P. Kratzer, M. Scheffler, and N. Moll, *Phys. Rev. Lett.* **82**, 4042 (1999).

<sup>17</sup>N. Combe, P. Jensen, and J.-L. Barrat, *Surf. Sci.* **490**, 351 (2001).

<sup>18</sup>V. A. Shchukin, N. N. Ledentsov, P. S. Kop'ev, and D. Bimberg, *Phys. Rev. Lett.* **75**, 2968 (1995).

<sup>19</sup>D. E. Jesson, G. Chen, K. M. Chen, and S. J. Pennycook, *Phys. Rev. Lett.* **80**, 5156 (1998).

<sup>20</sup>R. Koch, G. Wedler, J. J. Schulz, and B. Wassermann, *Phys. Rev.*

- Lett. **87**, 136104 (2001).
- <sup>21</sup>C. Ratsch, P. Šmilauer, D. D. Vvedensky, and A. Zangwill, *J. Phys. I* **6**, 575 (1995).
- <sup>22</sup>J. Drucker, *Phys. Rev. B* **48**, 18203 (1993).
- <sup>23</sup>M. Meixner, R. Kunert, and E. Schöll, *Phys. Rev. B* **67**, 195301 (2003).
- <sup>24</sup>K. Shorlin, M. Zinke-Allmang, and D. Fraser, *Phys. Rev. B* **66**, 165403 (2002).
- <sup>25</sup>C. Goyhenex and G. Tréglia, *Surf. Sci.* **446**, 272 (2000).
- <sup>26</sup>K. R. Heim, S. T. Coyle, G. G. Hembree, J. A. Venables, and M. R. Scheinfein, *J. Appl. Phys.* **80**, 1161 (1996).
- <sup>27</sup>A. B. Bortz, M. H. Kalos, and J. L. Lebowitz, *J. Comput. Phys.* **17**, 10 (1975).
- <sup>28</sup>V. I. Tokar and H. Dreyssé, *Phys. Rev. E* **68**, 011601 (2003).
- <sup>29</sup>M. Kästner and B. Voigtländer, *Phys. Rev. Lett.* **82**, 2745 (1999).
- <sup>30</sup>O. Diéguez, M. M. G. Alemany, C. Rey, P. Ordejón, and L. J. Gallego, *Phys. Rev. B* **63**, 205407 (2001).
- <sup>31</sup>J. A. Snyman and J. H. van der Merwe, *Surf. Sci.* **45**, 619 (1974).
- <sup>32</sup>J. H. van der Merwe and C. A. B. Ball, in *Epitaxial Growth, Part B*, edited by J. W. Matthews (Academic Press, New York, 1975), p. 493.
- <sup>33</sup>V. I. Tokar and H. Dreyssé, *TMS Lett.* **1**, 33 (2004).